

# IMPROVEMENT OF MECHANICAL PROPERTIES OF ALUMINA AND ZIRCONIA PLASMA SPRAYED COATINGS INDUCED BY LASER POST-TREATMENT

PAVEL CTIBOR, LADISLAV KRAUS\*, JARI TUOMINEN\*\*, PETRI VUORISTO\*\*, PAVEL CHRÁSKA

*Institute of Plasma Physics Academy of Sciences of the Czech Republic  
Za Slovankou 3, 180 00 Prague 8, Czech Republic*

*\*Research Center of Manufacturing Technology, Czech Technical University in Prague  
Horská 3, 128 00 Prague 2, Czech Republic*

*\*\*Institute of Materials Science, Tampere University of Technology, Tampere  
Korkeakoulunkatu 2, 33101 Tampere, Finland*

E-mail: ctibor@ipp.cas.cz

Submitted January 12, 2007; accepted September 21, 2007

**Keywords:** Plasma spraying, Laser post-treatment, Wear resistance, Al<sub>2</sub>O<sub>3</sub>, ZrO<sub>2</sub>

*Alumina and stabilized zirconia were plasma sprayed in air using a water-stabilized plasma torch. Nd-YAG laser was then used for additional treatment of the plasma sprayed coatings. The laser was maintained in a quasi-continual regime and defocused from the surface to increase the treated area. Energy density was varied together with the laser scanning velocity to ensure variance in thermal history of the treated surfaces. Microhardness, surface roughness and slurry abrasion resistance (SAR) were measured before and after the laser treatment. Results vary in dependence on the laser treatment parameters. When the laser treatment resulted in substantial changes of the structure (up to a complete re-melting of the surface), enhancement of all measured properties was proven. It is demonstrated that the change of the mechanical properties can be correlated with the optical properties of the coating materials at the laser wavelength. Microstructural aspects of the laser treatment are discussed as well, especially at the boundary between the laser-annealed layer and the basic coating. It is pointed out that laser remelting done by the use of a high energy density can cause presence of cracks, although the wear resistance as well as microhardness of the coatings is improved by this way. A cast ceramic material Eucor™ with the composition ZrO<sub>2</sub>-Al<sub>2</sub>O<sub>3</sub>-SiO<sub>2</sub> was treated by a diode laser utilizing the knowledge found on plasma coatings. The degree of improvement of the wear resistance, microhardness and homogeneity of microstructure was similar as in the case of plasma coatings.*

## INTRODUCTION

Plasma sprayed ceramic coatings for thermal barriers and wear protection often exhibit non-acceptable surface roughness and the cohesion and compactness of the surface layers are not sufficient. Also a decrease of the open porosity connected with the surface would be desirable to minimize the overall permeability of the coating for oxidizing agents etc.

The laser post-treatment of sprayed coatings ensures melting of the surface ceramic layer to a certain depth while, further below the surface, the layer remains unmelted and maintains the original coating structure. The top re-molten layer crystallizes rapidly after the laser has passed over it and the crystallization process is similar to the 'casting' of a ceramic melt onto a ceramic 'mould'. Fast nucleation is attained. Also the lamellar microstructure is destroyed and a new equiaxial dense crystal structure is established. Thermal stresses originating from cooling of the coating are relaxed and usually also the untreated part is relaxed but new thermal stresses are created by the laser treatment.

We can summarize that to a certain extent the laser-treated thermal spray coating can be regarded as a sandwich of two ceramic layers on a substrate.

Chemical homogeneity of the ceramic material is improved in the re-molten layer. Porosity decreases but new cavities and spherical bubbles are often present [1,2]. The reason is that gas bubbles, created during laser heating have not enough time to penetrate to the top of the melt before re-solidification. These bubbles are usually not interconnected and they do not penetrate through the whole coating. The laser-treated surface gives therefore a better corrosion protection of the substrate compared to the untreated one [3].

In the case of alumina, laser-treatment results in a change of  $\gamma$  phase in the treated coating to the stable  $\alpha$  phase [3-5]. The very low thermal conductivity of zirconia (2.2 W/mK for ZrO<sub>2</sub> stabilized by 8 wt.% of Y<sub>2</sub>O<sub>3</sub>) complicates heat removal from the re-molten zone and quenching stresses and vertical cracks often cause the coating integrity to deteriorate [6]. In general, however, both mentioned ceramics exhibit an improvement of microhardness after laser-treatment [3,4,7-9], which is,

in the case of alumina, further enhanced by the phase transformation. Porosity level decreases markedly [5,7,10]. According to the literature, a decrease of porosity and the absence of a dendritic structure in the re-molten zone is a sign of sintering in the laser treated layer [4]. But elsewhere, equi-axial dense crystal structure is reported as a sign of a complete remelting [3].

According to the literature, various lasers can be used for the post-treatment of thermally sprayed coatings. Nd-YAG laser is reported to be used at variety of energy densities from 0.2 up to 4 kJ/mm<sup>2</sup> [2]. CO<sub>2</sub> laser is usually operated around an energy density of 5 J/mm<sup>2</sup> [7,11] but also values as high as 37 J/mm<sup>2</sup> [12] or over 100 J/mm<sup>2</sup> are reported [2]. Excimer laser could be used at a very low energy density 0.02 J/mm<sup>2</sup> [10], as well as at very high power density 1 MW/mm<sup>2</sup> [9]. It is reported to melt zirconia and alumina coatings, respectively.

A typical treatment by a laser with an energy around 5 J/mm<sup>2</sup> produces: thickness of the layer with changed microstructure of approx. 100 μm [2,7,11], 25 % increase of microhardness for alumina [7], and a significant decrease of the porosity - almost to zero [7,8].

Fernandez et al. [7] report the microhardness of an alumina coating as HV<sub>0.3</sub> = 1161 before the laser-treatment and HV<sub>0.3</sub> = 1444 after it; other authors give HV = 940 before and 1400 after the treatment [9]. Abrasion resistance of laser-treated coatings has not been reported in detail, but an improvement after the treatment is pointed out [7,8,14]. An addition of titania into alumina is found to be advantageous for an increase of the wear resistance of the coating. It is important to note that TiO<sub>2</sub> reduces the hardness of these ceramic coatings [8]. Thermal shock resistance has also sometimes been the subject of research activities [9,15]. Aihua et al. [9] describe the thermal cycling of alumina-based coatings. Tendency for delamination was suppressed in the laser-treated samples compared to the as-sprayed ones. Thermal cycling up to 1270°C [15] is reported to show no improvement at treated vs. untreated coatings - either for alumina or zirconia.

Scattered reflectivity was studied by UV-VIS-NIR spectrophotometry [16]. An increase of reflectivity with increasing wavelength of the incident radiation was reported for the laser-treated stabilized zirconia. From

Table 1. Laser parameters.

Working wavelength (μm)	1.06
Power (kW)	2
Focus distance (mm)	55
Working distance (mm)	35
Beam width (mm)	10
Protective gas	Argon

the comparison of reported results, it is evident that zirconia is more sensitive to laser energy density; large cracks are much more typical for zirconia compared to alumina.

Objective of our paper is to demonstrate marked improvement of the wear resistance of plasma sprayed zirconia and alumina coatings attained via laser post-treatment. Similar effect was demonstrated also on a cast ceramic material Eucor™ containing high quantity of alumina and zirconia, whereas significantly lower time was dedicated to laser parameters optimization thank to the similarity of both experiments.

In all cases, attention is paid to microstructure of the material before and after treatment. Other characteristics as microhardness and surface roughness are mentioned.

## EXPERIMENTAL

### Samples manufacturing

Two types of coating materials were sprayed: YSZ zirconia - (ZrO<sub>2</sub> + 7.9 wt.% Y<sub>2</sub>O<sub>3</sub> + 0.01 wt.% SiO<sub>2</sub>) and grey Alumina - labelled "AG" (Al<sub>2</sub>O<sub>3</sub> + 4.7 wt.% TiO<sub>2</sub> + 1.4 wt.% Fe<sub>2</sub>O<sub>3</sub>).

Samples were manufactured using a high-throughput water-stabilized plasma spray system WSP® 500 (Institute of Plasma Physics, Prague, Czech Republic). This system operates at about 160 kW arc power and can process sufficient amounts of material per hour. The feeding distance for all samples was 24 mm; the spraying distance for AG were 300 and 400 mm while for YSZ only 300 mm. As substrates, flat carbon steel coupons were used. Substrate roughness was 8 ± 1 μm. The powder was carried in by compressed air through two injectors. Deposited coating thickness was about 1.5 mm.

Table 2. Labelling of the samples.

Sample label	Energy density <i>E</i> (J/mm <sup>2</sup> )	Laser scanning velocity <i>v</i> (mm/min)	Plasma spray distance <i>SD</i> (mm)
YSZ	-	-	300
YSZ 5	5	2400	300
YSZ 15	15	800	300
YSZ 20	20	600	300
YSZ 25	25	475	300
YSZ 30	30	400	300
AG 300	-	-	300
AG 300 6	6	2000	300
AG 400 6	6	2000	400
AG 300 7	7	1700	300
AG 400 7	7	1700	400
AG 400 8	8	1500	400

Nd-YAG laser (Institute of Materials Science, Tampere University of Technology, Finland) was used for additional treatment of plasma sprayed coatings. The laser was maintained in a quasi-continual regime and defocused from the surface to increase the treated coating's area. Table 1 summarizes laser working parameters. A special scanning head enabled continuous surface treatment when moved via manipulator.

Energy density  $E$  [ $\text{J}/\text{mm}^2$ ] and laser scanning velocity  $v$  [ $\text{mm}/\text{min}$ ] were varied to keep the product  $E \cdot v = \text{const.}$ , see Table 2. Lower energy at higher speed represents combination with a small effect on the sample surface while combination of higher energy at lower speed produces a large effect on the sample surface. Higher degree of melting attained by the high laser energy needs slower cooling to build a new surface with moderate surface roughness. Too rapid cooling, which will be induced e.g. by fast movement of laser head powered with high energy can lead to strongly uneven surface, similarly to [17]. Such a character of the surface is not advantageous for our general goal - improvement of the wear resistance.

Samples without indication of laser parameters are untreated (as-sprayed) coatings as reference materials.

The laser post-treatment of cast ceramics Eucor™ was carried out at Research Center of Manufacturing Technology, CTU in Prague, with a Rofin DL 031Q direct diode laser (Rofin - Sinar GmbH, Germany). To achieve maximum laser power, wavelengths 808 and 940 nm were used. The laser was equipped with wide rectangular beam geometry, similar to [18]. Theoretical specific energy applied on the treated surface was on the order of tens of joules per square millimeter. The laser traveling speed in range between 100 and 600 mm/min was tested.

Eucor™ is material containing about 14 wt.% of  $\text{SiO}_2$  and up to 2 wt.% of alkali-earth oxides in addition to the near-eutectic ratio of  $\text{Al}_2\text{O}_3$  and  $\text{ZrO}_2$  (alumina-zirconia pseudobinary, the system contains a eutectic point at 58 wt.%). This refractory material, called Eucor™ (EUTIT, Stara Voda, Czech Republic), is commercially available as cast tiles and linings and exhibits high hardness, high abrasion resistance, and extremely high chemical resistance. It is fabricated by melt casting followed by slow furnace cooling. It was confirmed by EDS that there are three chemically distinct regions within bulk. Pure phases of  $\text{Al}_2\text{O}_3$  and  $\text{ZrO}_2$  are accompanied by regions of mixed Al and Si oxides with traces of Na, K, and Ca [19]. The eutectic microstructure of the material is rather coarse (see Figure 7 -left) due to the slow furnace cooling after casting Eucor™ material.

#### Analytical techniques

A cross section of the substrate-coating system was cut by a low speed saw equipped with a diamond wheel

(Leco, USA) and then mounted in a resin. Standard grinding and polishing techniques were used for sample preparation.

Microstructure was studied using the light microscopy on polished cross sections. Micrographs were taken via CCD camera and via the image analysis (IA) software (Lucia G, Laboratory Imaging, Czech Rep.). Images of microstructures were taken from various areas of a cross section for each sample, especially at the interface between the laser-annealed layer and the untreated coating.

Microhardness was measured by the Hanemann microhardness head mounted on the light microscope with fixed load 1N (100 g) and the Vickers indenter. Minimum 10 indentations from various areas of a cross section for each sample were analyzed and average values with their standard deviations were calculated.

The most widely used parameter for evaluating the surface roughness is the mean arithmetic deviation of the profile  $R_a$ . This parameter  $R_a$  and the maximum height of profile  $R_v$  sufficiently classify the character of the relief. Both parameters were evaluated using roughness tester SURTRONIC 3P (Taylor Hobson, UK). The evaluated length was 25 mm and the results are averages from 5 measurements of different paths.

Slurry abrasion response of coatings was measured according ASTM standard [20]. SAR wear rate is determined by measuring the mass loss rate of a standard-shaped block when lapped in slurry. The test is run for 4 hours in 2-hour increments with mass loss being measured at the end of each 2-hour increment. The applied force was 22.24 N per specimen. After each 2-hour run the specimens were ultrasonically cleaned and weighted. The wear loss is expressed in grams per square centimeter instead of more frequently used volumetric units [19] because of lack of precise knowledge of specific weight of the basic coating and laser-treated zone. Accuracy of the measurement is approx.  $\pm 5\%$ .

Reflectivity of the coatings was measured by scanning UV-VIS-NIR spectrophotometer MPC 3100 (Shimadzu, Japan). The comparative reflectivity was measured at the wavelength of the laser used for the post-treatment, i.e. 1.06  $\mu\text{m}$ . As the standard barium sulfate was used with reflectivity independent of the used frequency ("100%").

## RESULTS AND DISCUSSION

### Structure and microhardness

As-sprayed zirconia coatings have uneven surface and contains a lot of pores and defects, Figure 1a. Average microhardness  $HV_{0.1}$  is 727 (see Table 3), which is lower than the microhardness of bulk YSZ [21]. Laser treatment leads to a significant increase of microhardness (over 50 %) for all used laser parameters. The

highest increase (60 %) was for sample YSZ 30 ( $HV_{m0.1} = 1793$ ), where energy density was the largest ( $30 \text{ J/mm}^2$ ). A very dense remolten layer with thickness over  $300 \mu\text{m}$  can be seen at the cross section. Although this layer exhibits sharp internal voids, the surface is flat - Figure 1d.

Samples YSZ 15 and YSZ 25 both exhibit also similar values of microhardness ( $1729 HV_{m0.1}$  and  $1717 HV_{m0.1}$  respectively; similar also to YSZ 30), represent-

ing an increase of 58 % in both cases. However, the microstructures are quite different: YSZ 15 has a clearly distinguishable dense remolten layer with an even surface. Thickness of this layer is approx.  $250 \mu\text{m}$ . Vertical cracks and local delamination of the glass-like surface layer are evident - Figure 1b. Sample YSZ 25 has the remolten layer with a varying thickness up to  $240 \mu\text{m}$ . Some vertical cracks are present but they do not go from one layer to the other one, see Figure 1c. On the contrary, sample YSZ 20 had only a thin remolten layer on the surface. The layer includes spherical pores and has very planar surface but the microhardness increase is less pronounced:  $1464 HV_{m0.1}$  (i.e. 50 % increase).

The as-sprayed grey alumina shows an uneven surface and contains many pores and defects, see Figure 2a. Its microhardness is  $HV_{m0.1} = 1515$ . As in the case of zirconia, alumina exhibits the highest increase of microhardness when laser-treated with the highest energy density ( $8 \text{ J/mm}^2$ ; Figure 2b). The microhardness of this sample (AG 400 8) reaches  $HV_{m0.1} = 2257$  (i.e. an increase of 33 %). The relative increase of the microhardness is lower compared to zirconia, probably due to the fact that the alumina is so hard material that further enhancement of its hardness is more limited. The

Table 3. Microhardness values.

Sample label	$HV_{m0.1}$	Standard deviation	Increase of $HV_{m0.1}$ (%)
YSZ	727	161	-
YSZ 5	n.a.	n.a.	n.a.
YSZ 15	1729	55	58
YSZ 20	1464	101	50
YSZ 25	1717	59	58
YSZ 30	1793	77	60
AG 300	1515	123	-
AG 300 6	1763	220	14
AG 400 6	1801	373	16
AG 300 7	1706	182	11
AG 400 7	2158	536	30
AG 400 8	2257	267	33

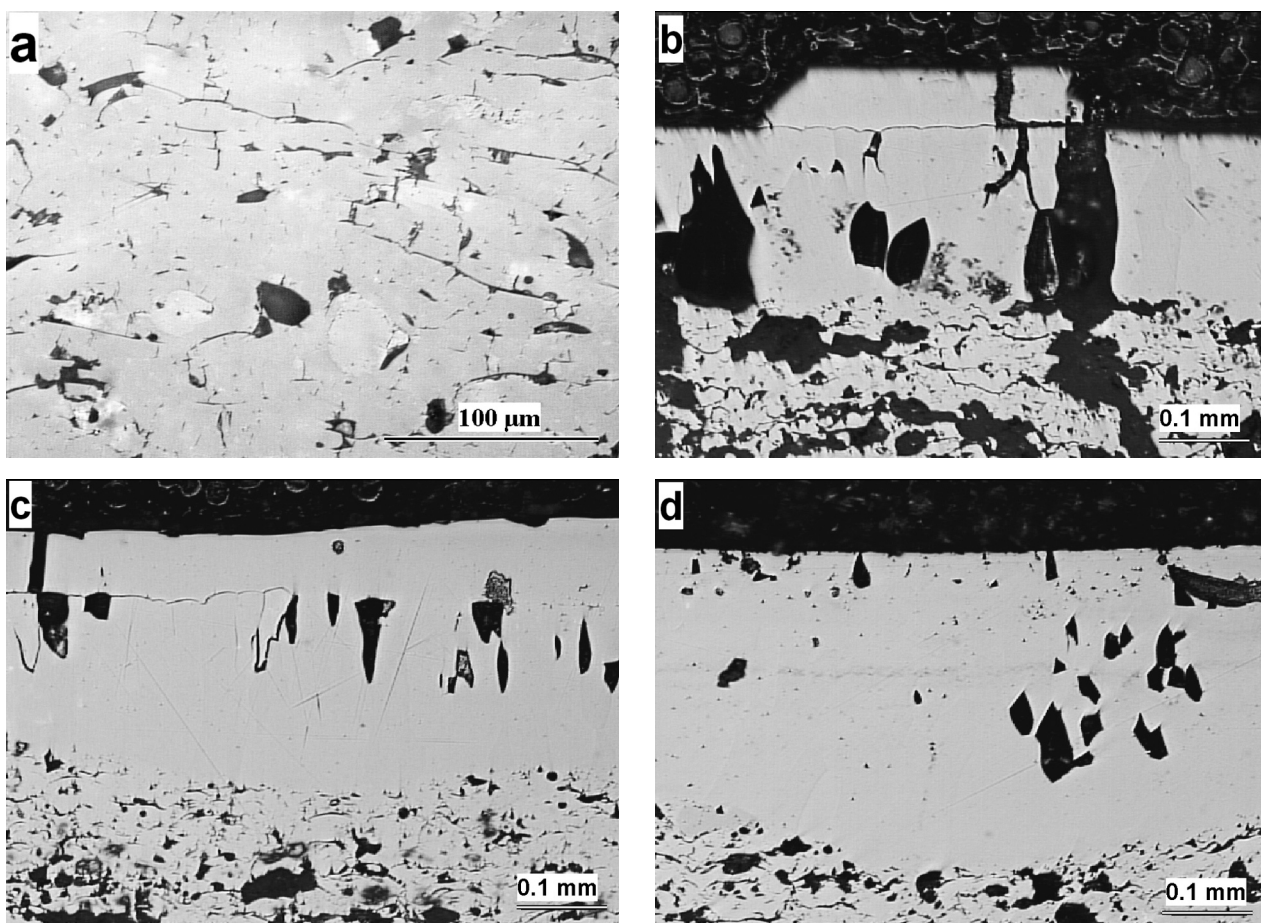


Figure 1. Microstructure of zirconia samples, light microscopy - a) YSZ, b) YSZ 15, c) YSZ 25, d) YSZ 30.

visual difference between the untreated layer and the laser-treated one is not very pronounced on micrographs (see Figure 2b). The remolten layer is around 80  $\mu\text{m}$  thick and contains closed and open spherical pores, however the total depth influenced by the laser is approx. 200  $\mu\text{m}$ . The laser-treated surface looks more even than the as-sprayed one.

Very similar increase of the microhardness is exhibited by the sample AG 400 7 (laser energy density 7  $\text{J}/\text{mm}^2$ , spray distance 400 mm). The cross-section

shows a 300-350  $\mu\text{m}$  thick laser-influenced layer consisting of two distinct parts. The remolten layer at the surface is fairly thin (50  $\mu\text{m}$ ), but the surface is more flat compared to the as-sprayed one. It contains many pores and defects with a different character from the following "bottom" part of the treated layer, such as some pores/bubbles open to the surface (see Figure 2f).

Sample AG 300 7 differs from AG 400 7 only by the spraying distance and it shows only 11 % increase in microhardness value ( $HV_{0.1} = 1706$ ). Cracks parallel

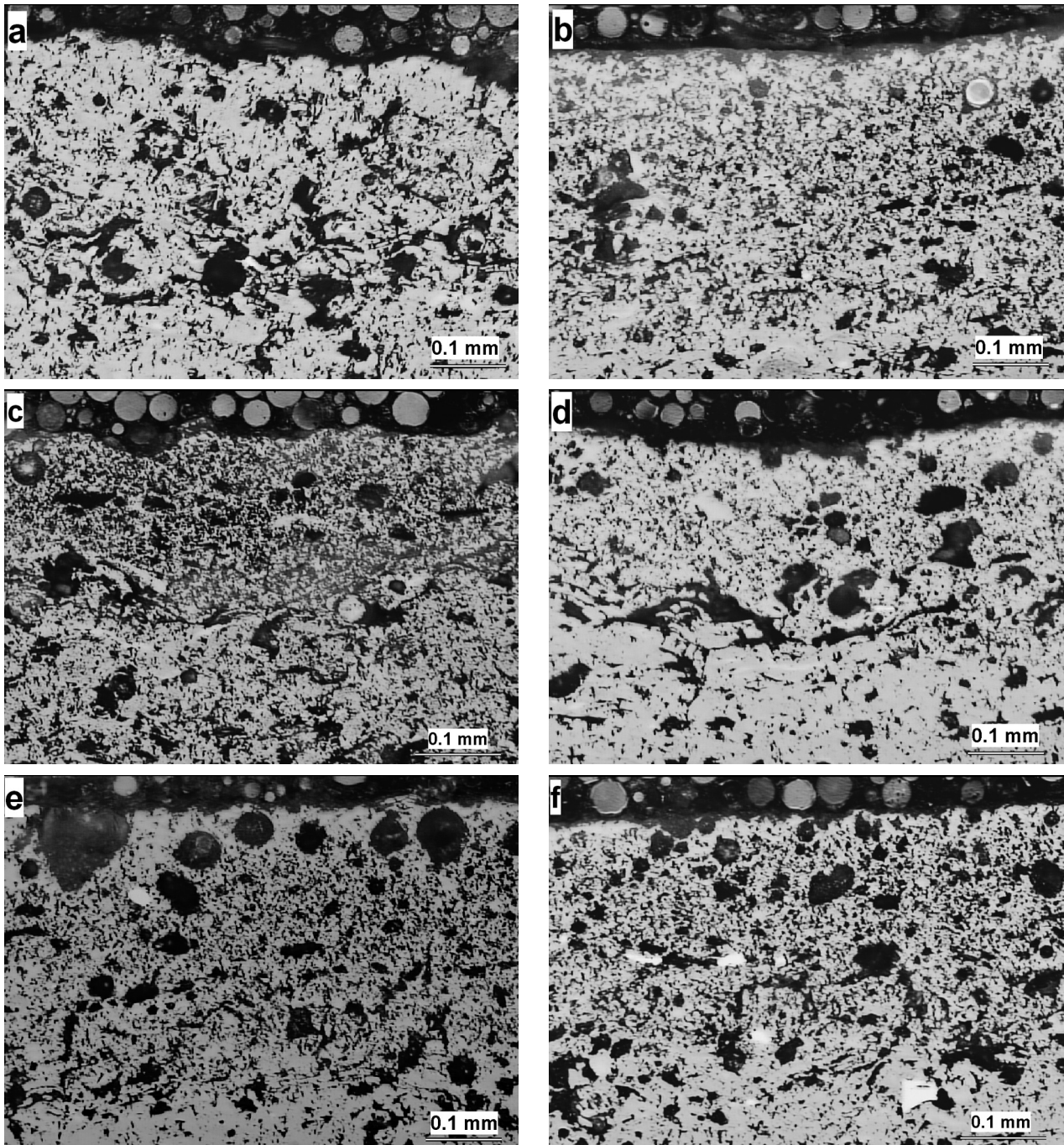


Figure 2. Microstructure of alumina samples, light microscopy, a) AG 300, b) AG 400 8, c) AG 300 6, d) AG 300 7, e) AG 400 6, f) AG 400 7.

with the surface are present at the interface between the treated and untreated part - Figure 2d. The top part contains some craters and the layer itself seems to be not completely remolten.

The hardness increase for samples AG 300 6 and AG 400 6 is approximately the same (1763 and 1801  $HV_{m0.1}$ , increase 14 and 16 %, respectively) and also the microstructures are similar. The laser-influenced layers are approx. 200  $\mu\text{m}$  thick (Figure 2c and 2e). At the interfaces between treated and untreated parts, certain presence of cracks parallel with the surface was detected. Defects from the laser-influenced layer are penetrating to the non-influenced part of the coating. Some craters are also on the surface. It is evident that the spray distance is without any substantial influence on the final microhardness.

### Surface roughness

Generally, the laser treated zirconia coatings are covered by a glass-like layer with many defects which are responsible for the increase of  $R_y$  and to a lower extent also  $R_a$  (see Table 4). Only sample YSZ 30, treated with the highest energy density, exhibits a decrease of both parameters  $R_a$  and  $R_y$ . Decrease of  $R_a$  is more pronounced and represents reduction almost to one half. Alumina laser treated coatings have lower roughness, as given by both parameters, compared to the as-sprayed coating. Influence of the spraying distance is insignificant.

### Wear resistance

Zirconia samples YSZ 5 and YSZ 15 exhibited a peculiar behavior: their wear loss after the first two cycles is higher than for the as-sprayed coatings, then their wear loss becomes lower. This can be probably explained by wearing-off the surface glass-like layer.

Table 4. Roughness values.

Sample label	$R_a$ ( $\mu\text{m}$ )	$R_y$ ( $\mu\text{m}$ )	Relative change of	
			$R_a$ (%)	$R_y$ (%)
YSZ	14.7	61.1	-	-
YSZ 5	15.6	103.1	5.77	40.74
YSZ 15	17.1	109.6	14.04	44.25
YSZ 20	12.6	111.9	-16.67	45.40
YSZ 25	15.0	100.6	2.00	39.26
YSZ 30	8.2	55.3	-79.27	-10.49
AG 300	19.7	121.1	-	-
AG 300 6	14.8	96.0	-33.11	-26.15
AG 400 6	15.0	103.2	-31.33	-17.34
AG 300 7	13.7	90.6	-43.80	-33.66
AG 400 7	15.0	100.4	-31.33	-20.62
AG 400 8	n.a.	n.a.	n.a.	n.a.

Sample YSZ 20 had a better wear resistance than the as-sprayed coating immediately from the beginning of the measurement. The slope of the linear fit of data is similar to YSZ 5 and 15, but the absolute values are lower.

Samples YSZ 25 and YSZ 30 (Figure 3) reveal much better wear resistance than the as-sprayed coatings. The slope of the linear fit is similar in both cases and increase of the wear loss with increasing length of the test path in the abrasive slurry is negligible compare to all previous samples. This fact corresponds to the dense glass-like layer on the top, which is hard and also exhibits an improved friction thanks to the lower surface roughness. The maximum change of the wear resistance is reached with the laser energy density increase to 25  $\text{J}/\text{mm}^2$  and further increase of the energy density does not change the wear loss values.

Alumina samples show a substantial enhancement of the wear loss behavior at all used combinations of the laser-treatment parameters. The slope of the linear fit (see Figure 4) is similar in all post-treated samples and increase of the wear loss with the length of the test path in the abrasive slurry is significantly reduced compared to the as-sprayed coatings. Higher laser energy density

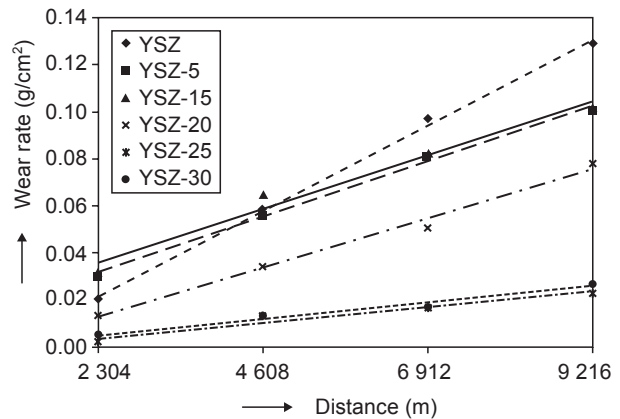


Figure 3. Wear rate of zirconia samples.

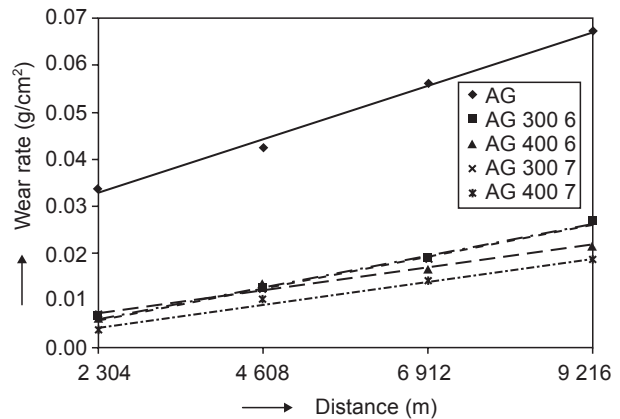


Figure 4. Wear rate of alumina samples.

causes slightly higher improvement of the wear resistance, but the difference is very small. Spray distance has practically no influence on the wear losses.

It is interesting to compare the absolute values of the wear losses for both tested materials. The as-sprayed

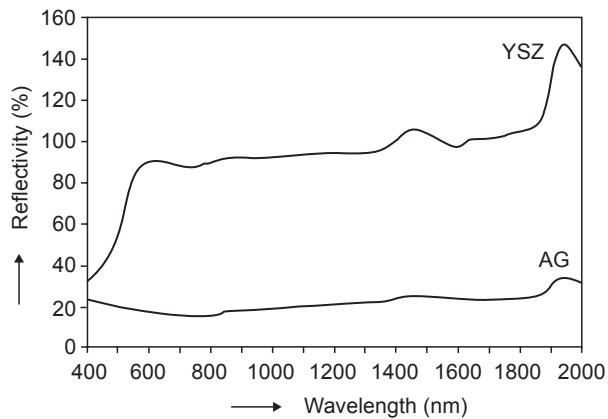


Figure 5. Reflectivity of zirconia (YSZ) and alumina (AG) plasma sprayed coating.

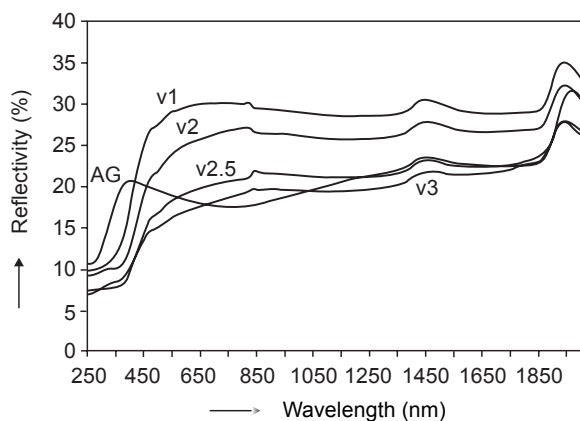


Figure 6. Reflectivity of alumina plasma sprayed coating without (AG) and with various laser post-treatments.

alumina has approximately two times better wear resistance than the as-sprayed zirconia. However, after 9 km long test path in abrasive slurry, values of the best laser treated samples are very similar. This finding suggests that the laser-induced enhancement of the wear resistance is two times higher for zirconia compared to alumina. Approx. five times higher energy density of Nd-YAG laser is for zirconia high enough to cause two times higher change of the wear resistance. Alumina is also a more effective absorbent of Nd-YAG laser energy than zirconia.

The previous results become clearer looking at results on the reflectivity measurements. On the Figure 5 curves of relative reflectivity of as-sprayed alumina and zirconia are given. At the wavelength of Nd-YAG laser (1060 nm) the reflectivity of zirconia is 92 compared to 20 for alumina. In other words, alumina absorbs 4.6 times higher portion of energy of incoming laser beam.

#### Optical properties and effectivity of laser treatment

Figure 6 shows reflectivity measurements done on white alumina plasma sprayed coating after laser treatment of various energy densities. This experiment was done in other laser beam geometry (not suitable for larger samples preparation) whereas only variable parameter was the laser scanning velocity - the number at each curve in the Figure 6 corresponds to velocity in [mm/s]. Main result of those measurements is the dependence of the reflectivity on laser energy density: the trend is clear - larger energy density (lower velocity) leads to reflectivity increase. It means that the 'relative effectivity' of the laser energy transfer to the alumina is highest for the 'virgin surface' (as-sprayed, AG in Figure 6) and decreases for once treated surface. This will play a role by e.g. a laying of adjacent scans at large area remelting by a laser with limited footprint size.

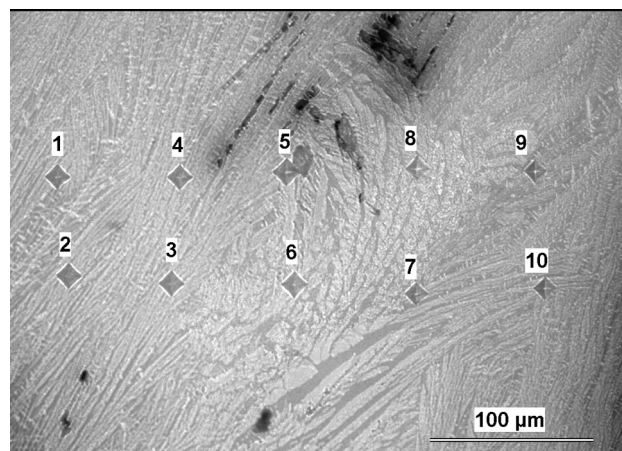
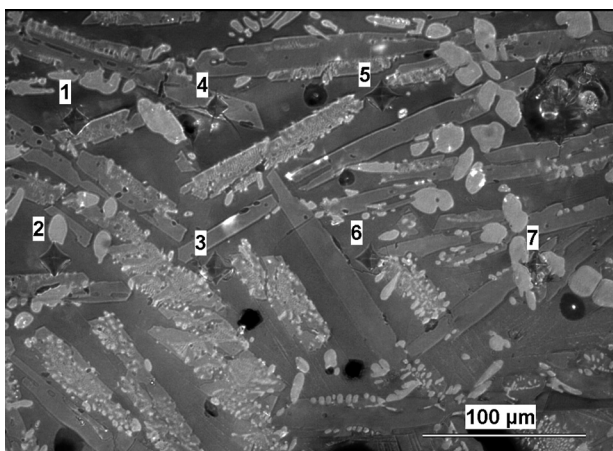


Figure 7. Cross section of cast Eucor™ with indents labeled by numbers (left) and indents in laser-remelted layer of the same material, light microscopy.

Structure and properties of cast ceramics treated by diode laser

Cross sections of the Eucor™ samples are shown in Figure 7. On the left is the bulk structure with needle-like rough crystals and smaller lighter islands - those features are connected with a variation in concentration of Al<sub>2</sub>O<sub>3</sub> and ZrO<sub>2</sub>, as found earlier [19]. Those two "phases" do not seem to have very different hardness (see Figure 7 left).

The new surface layer, though, is very dense and homogeneous structurally as well as mechanically (see Figure 7 right and Table 5). Dispersion of the microhardness in the laser post-treated zone is diminished.

Table 5. Mean microhardness and its standard deviation on studied Eucor™ samples.

Sample	Microhardness $HV_{m0.1}$	Standard deviation
Cast bulk	1218	330
Remelted layer	1375	159

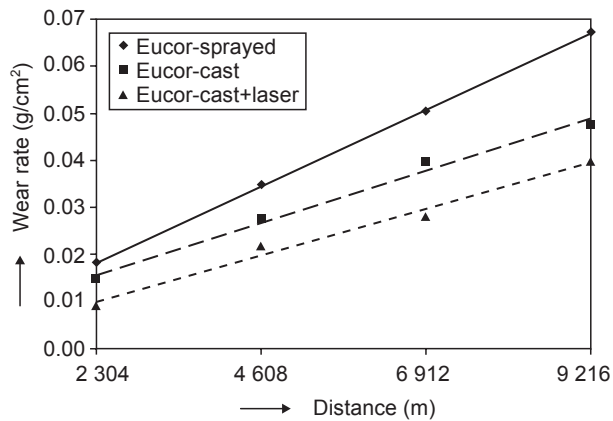


Figure 8. Wear rate of Eucor™ samples.

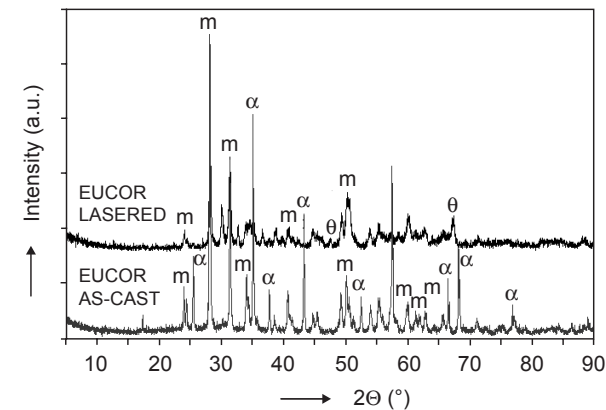


Figure 9. XRD patterns of Eucor™ samples (laser post-treated - top, cast material - bottom).

Figure 8 shows SAR test results as volume losses versus the distance passed in slurry. We see smaller losses for laser-treated samples that means improved wear resistance, although only slightly, of the laser-remelted surface. Plasma spraying of this material was performed as well [19], after crushing it to a powder. Although the coatings were amorphous and due to this fact their wear resistance was not well, see Figure 8. - The thickness of the remelted layer on the surface of as-cast samples was nearly 1 mm; also it is high enough to not be removed completely by the SAR test.

X-ray diffraction patterns (Siemens D500, Germany) of as-cast bulk Eucor™ and laser-treated one are displayed in the Figure 9. Tetragonal zirconia was detected in the laser-treated sample besides of monoclinic phase. Alpha alumina presented in as-cast material was recrystallized into theta phase. That should be the reason why the microhardness and also the wear resistance was increased only slightly - the effect of microstructural homogenization is an advantage but the phase transformation is a drawback.

CONCLUSIONS

Nd-YAG laser was used for additional treatment of plasma-sprayed coatings made from stabilized zirconia and grey alumina. Microhardness, surface roughness and slurry abrasion resistance (SAR) were measured before and after the laser treatment and enhancement of all measured properties was proven.

For zirconia, to improve the overall quality of the coating, high values of the energy density of the laser beam are the best. Such parameters are represented for example by sample YSZ 30. Increase of the laser energy density leads to an improvement of the wear resistance and microhardness. Integrity of the coating is although limited by formation of large horizontal cracks.

For alumina the microstructure of the laser-treated surface does not differ so markedly from the base coating. However, the studied range of the laser parameters was not so broad as in the case of zirconia and so far it can be concluded that all used parameters lead to a similar, moderate improvement of all tested properties. Structure of the coating seems to be acceptable for industrial applications, despite of variation in the spray distance at plasma spraying. To find useful laser parameter window and maintain the process for desired product properties is easier for grey alumina than for stabilized zirconia.

Quality of alumina and zirconia plasma-sprayed coatings produced by water-stabilized plasma torch could be improved significantly by laser after-treatment of the surface using Nd-YAG laser.



Cast ceramics was post-treated with a diode laser using similar setup and energy impact comparable with the plasma sprayed samples. The increase of microhardness and wear resistance was confirmed also in this case, despite of unfavourable transformation in alumina phase.

#### Acknowledgement

The Czech authors acknowledge support of the Academy of Sciences of the Czech Republic under project CV IQS 200430560.

#### References

1. Chang, K. C., Wei W. J., Chen C.: Surf. and Coat. Technol. 102, 197 (1998).
2. Ilyushenko A. P., Okovity V. A., Tolochko N. K., Steinhauer S.: Mat. Manuf. Proc. 17, 157 (2002).
3. Aihua W., Zengyi T., Beidi Z., Jingmin F., Xianyao M.: Surf. and Coat. Technol. 52, 141 (1992).
4. Krishnan R., Dash S., Babu Rao C: Scripta Materialia 45, 693 (2001).
5. Krishnan R., Dash S., Sole R., Tyagi A., Ray B.: Surface Eng. 18, 208 (2002).
6. Chen H. C., Pfender E., Heberlein J.: Thin Solid Films 315, 159 (1998).
7. Fernandez, E., Cuetos J. M., Vijande R., Rincon A.: Tribology International 29, 477 (1996).
8. Yuangzheng Y., Youlan L., Zhengyi L., Yuzhi Ch.: Mat. Sci. Eng. A 291, 168 (2000).
9. Aihua W., Beidi Z., Zengyi T., Xianyao M., Shijun D., Xudong Ch.: Surf. and Coat. Technol. 57, 169 (1993).
10. Liu Z.: Appl. Surf. Sci. 186, 135 (2002).
11. Tsai H. L., Tsai P. C.: J. Mat. Eng. and Perf. 7, 258 (1998).
12. Khor K. A., Jana S.: J. Mat. Proc. Technol. 66, 4 (1997).
13. Gravanis G., Tsetsekou A., Zambetakis Th., Stouranas C.: Surf. and Coat. Technol. 45, 245 (1991).
14. Fu Y., Batchelor A. W., Xing Y., Gu Y.: Wear 210, 157 (1997).
15. Pawlowski L. in: Proc. of the International Thermal Spray Conf. 2002, p. 721 - 726, Ed. C. Berndt, ASM International, Materials Park, Ohio 2002.
16. Chwa S. O., Ohmori A.: Surf. and Coat. Technol 148, 88 (2001).
17. Thomas G., Grant P.S., Coad P., Matthews G., Castro R. in: Proc. of International Thermal Spray Conf. 2006, Seattle, Ed. C. Berndt, ASM International, Materials Park, Ohio 2006.
18. Tuominen J., Latokartano J., Vihinen J., Vuoristo P., Mantyla T. in: Proc. of International Thermal Spray Conf. 2006, paper s13-5-11362, Seattle, Ed. C. Berndt, ASM International, Materials Park, Ohio 2006. paper s13-5-11362.
19. Chraska T., Neufuss K., Dubsy J., Ctibor P., Rohan P.: Bulk nanocrystalline alumina-zirconia materials, Accepted for publication by Ceramics International.
20. ASTM G 75 - 01: Standard Test Method for Determination of Slurry Abrasivity (Miller Number) and Slurry Abrasion Response of Materials (SAR Number), ASTM International, West Conshohocken, PA, USA.
21. Kalinovic D.F., Kuznecova L.I., Denisenko E.T.: Powder metallurgy (Poroshkovaya metallurgija) 11, 98 (1987).

#### ZLEPŠENÍ MECHANICKÝCH VLASTNOSTÍ PLAZMOVÝCH NÁSTRÍKŮ OXIDU HLINITÉHO A OXIDU ZIRKONIČITÉHO DOSAŽENÉ POMOCÍ NÁSLEDNÉHO OVLIVNĚNÍ LASEREM

PAVEL CTIBOR, LADISLAV KRAUS\*,  
JARI TUOMINEN\*\*, PETRI VUORISTO\*\*,  
PAVEL CHRÁSKA

Ústav fyziky plazmatu AVČR  
Za Slovankou 3, 180 00, Praha 8

\*Výzkumné centrum pro strojírenskou technologii ČVUT  
Horská 3, 128 00, Praha 2

\*\*Ústav materiálových věd,  
Tampere University of Technology, Tampere,  
Korkeakoulunkatu 2, 33101 Tampere, Finsko

Oxid hlinitý a oxid zirkoničitý byly plazmově naneseny na podložky pomocí vodou stabilizovaného plazmatronu. Následně byl povrch těchto nástříků ovlivněn pomocí Nd-YAG laseru. Laser byl provozován v kvazi-kontinuálním režimu a zaostřen mimo povrch vzorku, aby se zvětšila plocha jeho stopy. Hustota energie laseru a rychlost jeho přejezdu nad vzorkem byly měněny tak, aby vznikla sada vzorků s odlišnou historií průběhu tepelného ovlivnění. Před laserovým ovlivněním a po něm byly měřeny mikrotvrdość, drsnost povrchu a odolnost proti opotřeby v suspenzi (SAR test). Pokud laserové ovlivnění vedlo k zřetelné změně mikrostruktury (až po její úplné přetavení), vždy bylo prokázáno i zlepšení sledovaných vlastností. Je ukázáno, že změny mechanických vlastností mají vztah k optickým vlastnostem ovlivňovaného materiálu při vlnové délce použitého laseru. Vedle vlastností jsou diskutovány i změny v mikrostrukturu laserem ovlivněné vrstvy vůči původní strukturu plazmových nástříků. Za podobného technologického režimu byl diodovým laserem ovlivněn lité keramický materiál EucorTM o složení  $ZrO_2-Al_2O_3-SiO_2$ , kdy byly uplatněny poznatky z ovlivnění plazmových nástříků. Došlo k obdobnému zlepšení oteruvzdornosti, mikrotvrdości a strukturální homogenity jako v případě plazmových nástříků.